V. Conclusion

The foregoing analysis indicates the importance of diffusion direction on the linearized mixing process within the diffuser. The same effect may be of even greater importance in the nonlinear case and should be examined both theoretically and experimentally.

References

[1] Quinn, B., "Compact Ejector Thrust Augmentation," *Journal of Aircraft*, Vol. 10, Aug. 1973, pp. 481–486.

[2] Pai, S. I. and Hsieh, T. Y., "Linearized Theory of Three-Dimensional, Jet Mixing With and Without Walls," *Journal of Basic Engineering*, Vol. 92, March 1970, pp. 93–100.

[3] Pai, S. I. and Hsieh, T. Y., "Three-Dimensional Laminar Jet Mixing," *Physics of Fluids*, Vol. 12, April 1969, pp. 936–938.

[4] Wolf, S. and Johnston, J. P., "Effect of Nonuniform Inlet Velocity Profiles on Flow Regimes and Performance in Two Dimensional Diffusers," *Journal of Basic Engineering*, Vol. 91, Sept. 1969, pp. 462–474.

Rocket Plumes in the Thermosphere

JAMES STARK DRAPER* AND FRITZ BIEN†
Aerodyne Research, Inc., Burlington, Mass.

AND

ROBERT E. HUFFMAN‡ AND DUANE E. PAULSEN§
Air Force Cambridge Research Laboratories, Bedford, Mass.

Nomenclature

F = missile thrust
$\bar{L} = [F/q_\infty]^{1/2}$ = hypersonic plume scale
$Kn_{\bar{L}} = \lambda_\infty/\bar{L}$ = plume Knudsen number
$q_\infty = \rho_\infty u_\infty^2/2$ = freestream dynamic pressure
u_∞ = freestream speed
λ_∞ = freestream mean freepath
ρ_∞ = freestream density

Introduction

TO provide correct freestream conditions for study of aerodynamic phenomena in the thermosphere (that part of the atmosphere above 90 km altitude), the time-varying properties of the thermosphere must be determined. By maintaining a fixed exospheric temperature of about 1500K as characterizing a "nominal" thermosphere, the standard atmosphere[1] does not allow for these constantly changing thermospheric property altitude profiles. One type of aerodynamic flow frequently studied in the thermosphere is that of rocket exhaust plume. The large property variations away from "nominal" thermospheric conditions can be used to explain the results of recent observations of a vehicle under rocket power in the thermosphere. It will be shown that to understand these observations, the state of the thermosphere must be established through knowledge of the simultaneous solar flux at 10.7 cm and the geomagnetic planetary index, the geographical subpoint and the local solar time, and the day of the year.

Received August 12, 1974; revision received December 5, 1974. This work is a part of Project Chaser, and was monitored by the Air Force Cambridge Research Laboratories under Contract F04611-73-C-0048. The Contract Monitor was D. E. Paulsen. Particular thanks for assistance are given to E. Powers of Aerodyne Research, Inc.

Index categories: Jets, Wakes, and Viscid-Inviscid Flow Interactions; Supersonic and Hypersonic Flow; Atmospheric, Space, and Oceanographic Sciences.

* Principal Research Scientist. Member AIAA.
† Research Scientist.
‡ Supervisory Research Chemist.
§ Research Chemist.

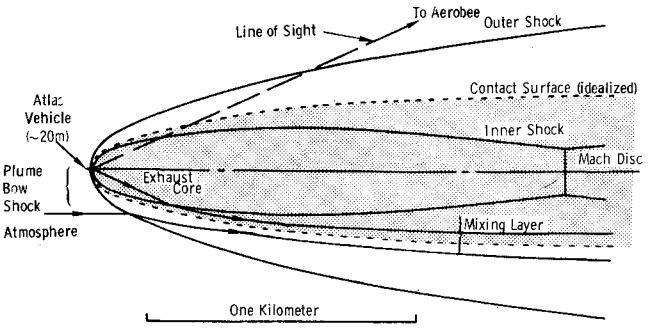

Fig. 1 Schematic of Atlas exhaust plume in the lower thermosphere at an altitude of 100 km showing a representative line of sight to the Aerobee Instrument Package.

Field Measurements

Recently, the Air Force Cambridge Research Laboratories (AFCRL) conducted Project Chaser, a program for the measurement of rocket plumes. Observations of an Atlas-103F vehicle launched at Vandenberg Air Force Base were made on one flight. The AFCRL instrument package, carried by an Aerobee 170 sounding rocket that followed the Atlas vehicle, contained a spatially resolving, ultraviolet photometer. This photometer viewed the Atlas rocket exhaust plume roughly from behind, as shown in Fig. 1. The photometer data has been analyzed to

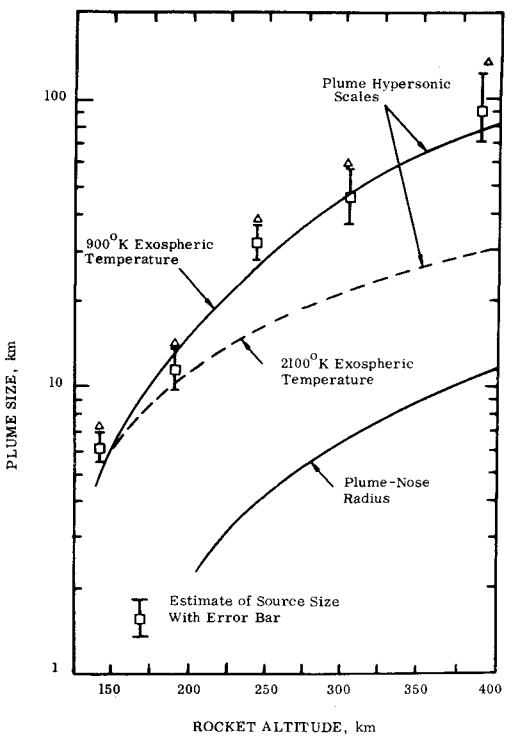

Fig. 2 The size of the observed radiation source vs Atlas altitude. As explained in the text the radiation source was initially assumed to be located at the vehicle, as shown by △. Subsequent analysis shows that the radiation source is probably closer to the plume Mach disk, as shown by the □, to which the error bars have been attached. A comparison is made of the size of the radiation source with the theoretical rate of growth of: 1) the plume mixing layer in "hot" (2100K) and "cold" (900K) exospheric temperature thermospheres; and 2) the growth of the plume bow shock in a 900K exospheric temperature thermosphere.

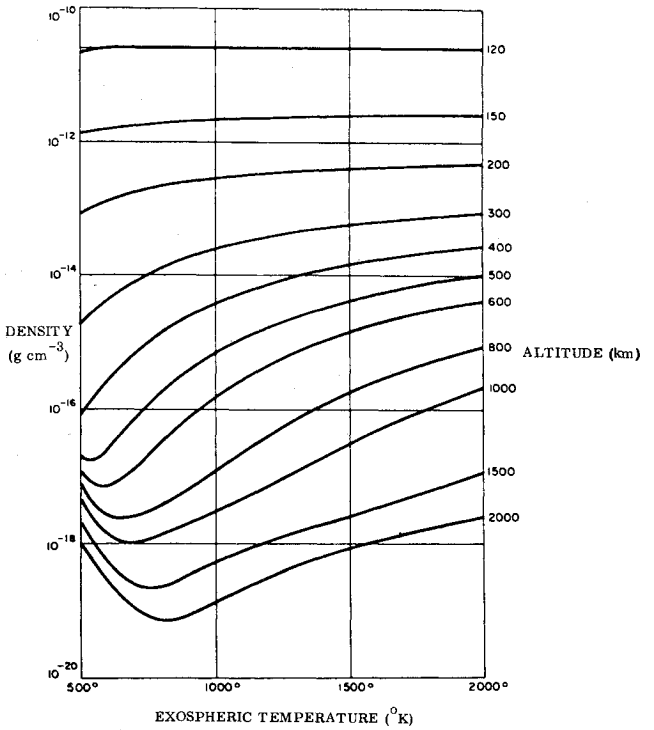

Fig. 3 Sensitivity of densities in the thermosphere to variations in exospheric temperature.[6]

provide a history of the size (at the vehicle location) of the observed radiating source. This source size history is shown by the triangles plotted vs vehicle altitude in Fig. 2.

Potentially one or more of four radiation sources might be observed: reflection from the vehicle body; hot exhaust core gases; hot plume bow-shock gases; and chemiluminescence in the plume mixing layer. Only the two latter sources, being associated with the rocket plume, will grow in size as the vehicle climbs to higher altitudes. The size of a rocket plume in a hypersonic ambient grows with the hypersonic plume scale $\bar{L} = (F/q_\infty)^{1/2}$, as is well established by theory[2,3] and experiment.[4] Here F is rocket thrust and q_∞ is dynamic pressure. Using $\bar{L}$ both the plume bow-shock diameter and the plume mixing-layer diameter sizes can be calculated.[5] The size histories of these regions for the Atlas vehicle are shown by the solid lines in Fig. 2. The data are clearly associated with both the size and growth of the plume mixing layer.

The mixing-layer radiation is extensive radially as shown in Fig. 2. It is also extensive axially, as inferred from its radial extent and the fact that its magnitude decayed only slowly upon engine shutdown. Therefore, the bulk of the observed radiation certainly originates from some point between the Atlas and the photometer. Since the radial spatial extent of the radiation source is established using the angle intercepted by the observed source and its presumed range along the line of sight, a shift in source position toward the photometer (since these are tail aspect measurements) has the effect of reducing estimates of the radiation source size. To estimate the rough magnitude of this effect, it will be assumed that the radiation centroid is located at the same plume axial station as the plume Mach disk (see Fig. 1). The source size measured then decreases somewhat as indicated by the open squares in Fig. 2. Altogether the agreement with the growth of the plume mixing layer in the 900K exospheric temperature thermosphere is quite good.

Thermospheric Model

Rocket thrust, trajectory, and ambient density are required to calculate the dimensions of the high altitude hypersonic plume. The ambient density depends upon the thermospheric state which is expressed through use of the exospheric temperature. Solar activity, local time, and geographic location can be used to evaluate the local exospheric temperature. The sensitivity of thermospheric density profiles to exospheric temperature is seen in Fig. 3 where ambient density has been plotted vs exospheric temperature by Jacchia.[6] An exospheric temperature of about 1500K characterizes the "standard" atmosphere.[1] In periods of high solar activity the exospheric temperature can approach 2000K. At a given altitude, density varies relatively little as exospheric temperature rises from 1500K to 2000K. However, in periods of low solar activity, when exospheric temperature may drop to 500K, there results an order of magnitude decrease in ambient density at an altitude of 400 km.

Table 1 Exospheric temperature estimation

Missile launched at Vandenburg Air Force Base on June 29, 1971		
Latitude	= 34.6 deg N	
Longitude	= 121.0 deg W	
10.7 cm Flux[a]	$F_{10.7}$	= 141.1 10^{-22} w/m^2/Hz
	$\bar{F}_{10.7}$	= 112.8 10^{-22} w/m^2/Hz
Geomagnetic Planetary Index[a]	A_p	= 18.0
Day 180		
Hour is 0312 o'clock LST		
Exospheric Temperature = 906.4K		

[a] Data from Ref. 5.

To estimate the exospheric temperature during the Atlas flight the approach described in the 1966 Supplements of the U.S. Standard Atmosphere[7] is used. Using the launch time solar and geophysical activity data[8] summarized in Table 1, the mean exospheric temperature for the high altitude portion of the Atlas trajectory was about 906K. The nearest thermosphere model, for an exospheric temperature of 900K,[7] was used to calculate the plume growth rates shown in Fig. 2. The thermosphere in the "standard" atmosphere would result in significantly slower plume growth as suggested by the dashed curve labeled 2100K in Fig. 2. The correspondence between the 1500K and 2100K thermospheres can be seen in Fig. 3. Below 400 km altitude there are only small differences in densities at a fixed altitude for 1500K and 2100K exospheric temperatures. Use of a "nominal" (1500K) thermosphere model would have posed serious problems of interpretation by requiring a rocket related source three times larger than the entire plume diameter. That the observed dimensions are slightly larger than the calculated mixing-layer diameter may partly be explained by the fact that foreshortening of the plume shape is not complete, as the photometer does not view the plume exactly from the tail, but rather from an oblique angle where some of the plume structure smears out the radiation image. The fact remains that when correct thermospheric and viewing geometry conditions are rigorously applied there results a good agreement between the observed radiation source and the plume mixing-layer behavior.

Conclusions

Calculations of hypersonic rocket plume structures in the thermosphere require rigorous incorporation of the thermosphere state using knowledge of solar and geophysical activity, local time and geographical location of the missile. Only by use of this approach can the extremely large radiation region seen in the recent AFCRL measurement of a rocket plume flying through an unusually cold thermosphere be satisfactorily explained. The effect of changing thermospheric states on rocket plume structures was originally pointed out by Draper and Moran[4] and subsequently included in the high-altitude plume nomogram of Draper and Sutton.[5] Because of the continuous worldwide surveillance of solar activity and the relatively good correlation between solar activity and thermospheric densities achieved by recent thermosphere models[6] (down to periods of several hours)

determination of the proper state of the thermosphere poses no fundamental obstacle to studies of aerodynamic structures in the thermosphere.

References

[1] *1962 U.S. Standard Atmosphere,* U.S. Government Printing Office, Washington, D.C., 1962.

[2] Alden, H. L. and Habert, R. H., "Gasdynamics of High Altitude Rocket Plumes," MITHRAS Rept. MC-63-80-R1, July 1964.

[3] Jarvinen, P. O. and Hill, J. A. F., "Universal Model for Underexpanded Rocket Plumes in Hypersonic Flow," 12th JANNAF Liquid Propulsion Meeting, Las Vegas, Nevada, Nov. 1970.

[4] Draper, J. S. and Moran, J. P., "A Study of Wind Tunnel Simulation of High Altitude Rocket Plumes," Tech. Rept. TR-72-111, Feb. 1973, Air Force Rocket Propulsion Laboratory (AFRPL), Edwards Air Force Base, Calif.

[5] Draper, J. S. and Sutton, E. A., "A Nomogram for High-Altitude Plume Dimensions," *Journal of Spacecraft and Rockets,* Vol. 10, Oct. 1973, pp. 682–684.

[6] Jacchia, L. G., "Revised Static Models of the Thermosphere and the Exosphere with Empirical Temperature Profiles," Special Rept. 332, May 1971, Smithsonian Astrophysical Observatory, Washington, D.C.

[7] *U.S. Standard Atmosphere Supplements, 1966,* Washington, D.C., 1966.

[8] *Solar-Geophysical Data* (Prompt Reports), No. 324-PART I, Aug. 1971, U.S. Department of Commerce, National Oceanic and Atmospheric Administration, Environmental Data Service, Washington, D.C.

Performance of the "Direct Search Design Algorithm" as a Numerical Optimization Method

MICHAEL PAPPAS*

New Jersey Institute of Technology, Newark, N.J.

Introduction

MATHEMATICAL programing (MP) optimization procedures have broad applicability in engineering and have found increasing acceptance in many areas. Such procedures, by means of an optimal search strategy, solve, or attempt to solve the problem: Find those values $\bar{x}_n$ of the variables x_n that minimize (or maximize) the "objective" function $f(x_n)$. That is, find

$$f(\bar{x}_n) = \min[f(x_n)] \tag{1}$$

Often the solution is constrained by one or more relations that can be written in the form

$$g_j(x_n) \leqq 0 \qquad j = 1,2,\ldots J \tag{2}$$

Constrained linear problems can be solved efficiently and reliably. Nonlinear problems are, in contrast, generally quite difficult and, in fact, no method exists that will guarantee a solution to the general constrained nonlinear MP problem.

Still, many algorithms for the solution of nonlinear problems have been proposed and successfully applied. The Direct Search Design Algorithm (DSDA), is a constrained nonlinear, mathematical programing procedure, proposed for the automated optimal synthesis of structures, which has been successfully applied to a number of structural problems.[1-4] Since the method has worked well in several applications the question arises: How does the DSDA compare with other nonlinear techniques that have also been successfully used for engineering design?

An excellent recent study by Eason and Fenton[5] evaluating the performance of seventeen different optimization codes on ten constrained nonlinear problems, provides a convenient benchmark against which the DSDA can be compared. This paper, therefore, attempts to provide an answer to the previous question by extending the work of Eason and Fenton to include an evaluation of the performance of the DSDA on these same problems.

Study and Results

A general FORTRAN IV code based on the DSDA using the original variable step pattern search, penalty function, and optimality check described in Ref. 1 was employed in this study. A similar code was also used for the study described in Ref. 6. This code requires the user to supply only the objective and constraint functions, although the convergence criteria and initial step size may also be specified. If no step size is specified a step size is internally generated.

All ten problems of Refs. 5 and 7 were run with the DSDA code from the starting points specified in these references. The internally generated step sizes were used for all problems and no algorithm control constants were changed during the study. Thus there was no tuning of the code to individual problems. All problems were run on an IBM 370 model 91 using the "G" level compiler and single precision.

Table 1 briefly describes the codes studied in Refs. 5 and 7 with the addition of the DSDA studied here. Additional details on these codes can be found in Refs. 1, 5, and 7. Table 2 presents results of the performance of these codes on the ten test problems in the form of a success matrix. The numerical entries indicate the normalized time required for solution,[5] the symbol P indicates progress toward a solution and a blank indicates failure. Definitions of "solution" and "progress" vary for each problem and are given in Ref. 7 as well as a detailed description of each problem.

Table 1 Code descriptions

Name	Description	Algor class[a]
ADRANS	Random search followed by pattern moves	DS
CLIMB	Rosenbrock search	DS
DAVID	Davidon-Fletcher-Powell with numerical derivatives	GF
DFMCG	Fletcher-Reeves conjugate gradient method with secant approximation derivatives	G
DFMFP	Davidon-Fletcher-Powell with secant approximation derivatives	G
FMIND	Hook & Jeeves pattern search	DS
GRAD4	Steepest descent method	G
GRID1	Grid and star network search, with shrinkage	AR
MEMGRD	Davidon-Fletcher-Powell with retained step length information	GF
NMSERS	Simplex search	DS
PATSH	Modified pattern search	DS
PATRN0	Modified pattern search, dome strategy	DS
PATRN1	Modified pattern search, ridge strategy	DS
RANDOM	Random search with shrinkage	AR
SEEK1	Pattern search followed by random search	DS
SEEK3	Modified pattern search	DSF
SIMPLX	Modified simplex search	DSF
DSDA	Modified pattern search followed by Mugele's search	DS

[a] DS = direct search, DSF = direct search employing SUMT strategy and penalty function, G = gradient procedure, GF = gradient procedure using SUMT strategy and penalty function, AR = area reduction method.

Received September 19, 1974. Grateful acknowledgement is given to Y. Moradi, a graduate student, for his efforts in helping prepare and run the problems of this study.

Index categories: Computer Technology and Computer Simulation Techniques; Structural Design, Optimal.

* Associate Professor, Mechanical Engineering Department. Member AIAA.